6-2013

Block Copolymer Self-Assembled and Cross-linked Nanoassemblies for Combination Delivery of Iron Oxide and Doxorubicin

Daniel Scott
University of Kentucky

Yihwa Beabout
University of Southern Indiana

Robert J. Wydra
University of Kentucky, wydrar@gmail.com

Mo Dan
University of Kentucky, mo.dan@uky.edu

See next page for additional authors

Authors
Daniel Scott, Yihwa Beabout, Robert J. Wydra, Mo Dan, Robert A. Yokel, J. Zach Hilt, and Younsoo Bae

Block Copolymer Self-Assembled and Cross-linked Nanoassemblies for Combination Delivery of Iron Oxide and Doxorubicin

Notes/Citation Information
Published in the *Journal of Applied Pharmaceutical Science*, v. 3, no. 6, p. 21-28.

Digital Object Identifier (DOI)
http://dx.doi.org/10.7324/JAPS.2013.3604

Journal of Applied Pharmaceutical Science Vol. 3 (06), pp. 021-028, June, 2013
Available online at http://www.japsonline.com
DOI: 10.7324/JAPS.2013.3604
ISSN 2231-3354 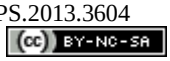

Block Copolymer Self-assembled and Cross-linked Nanoassemblies for Combination Delivery of Iron Oxide and Doxorubicin

Daniel Scott[1], Yihwa Beabout [2], Robert J. Wydra [3], Mo Dan [1,4], Robert Yokel [1,4], J. Zach Hilt [3] and Younsoo Bae [1]*
[1]Department of Pharmaceutical Sciences, University of Kentucky, Lexington, KY, USA.
[2]Department of Chemistry, University of Southern Indiana, Evansville, IN, USA.
[3]Department of Chemical and Materials Engineering, University of Kentucky, Lexington, KY, USA.
[4]Graduate Center for Toxicology, University of Kentucky, Lexington, KY, USA.

ARTICLE INFO

Article history:
Received on: 08/03/2013
Accepted on: 11/06/2013
Available online: 27/06/2013

Key words:
Nanoassemblies, nanoparticle, block copolymers, drug delivery, controlled release, iron oxide.

ABSTRACT

We describe the development of nanoscale polymer drug carriers for the combinational delivery of an anticancer drug (doxorubicin: DOX) along with super paramagnetic iron oxide nanoparticles (IONPs). The drug molecules were electrostatically loaded into both block copolymer self-assembled nanoassemblies (SNAs) and cross-linked nanoassemblies (CNAs). Both nanoassemblies entrapped DOX and IONPs either individually or in tandem, maintaining sub-100 nm diameter. The IONP-loaded nanoassemblies generated heat in the presence of an alternating magnetic field (AMF). Incorporation of the drug payload, DOX, showed no adverse effects on the heating profile. Drug release from the SNAs and CNAs was accelerated as temperature increased from the normal body temperature (37°C) to a mild hyperthermic condition (40 ~ 42°C). CNAs released DOX faster than SNAs regardless of an incubation temperature. CNAs co-entrapped IONPs and DOX were more stable than SNAs in aqueous solutions for five days. These results suggest that block copolymer cross-linked nanoassemblies provide viable delivery platforms for combination delivery of inorganic molecules, anticancer drugs, and potentially other various biologically active substances.

INTRODUCTION

Polymer nanoassemblies, molecular complexes typically prepared from biocompatible block copolymers, are widely used in current cancer research as drug carriers that can circulate in the body for a prolonged period of time and accumulate in tumor tissues efficiently (Ishida *et al.,* 1999; Lee *et al.,* 2010). Previous studies have demonstrated that spherical polymer nanoassemblies, 20 ~ 200 nm vesicles and particles, can entrap various molecules for diagnosis, imaging, and treatment of cancer (Bae *et al.,* 2009; Khemtong *et al.,* 2009; Torchilin 2011). In comparison to conventional anticancer therapy with small molecules (< 1,000 Da), chemotherapy using polymer nanoassemblies as drug carriers can reduce non-specific drug distribution in normal tissues by increasing the concentration of drug payloads preferentially in tumors (Matsumura *et al.,* 1986; Maeda *et al.,* 2000). Polymer nanoassemblies are also shown to overcome other pharmaceutical obstacles for anticancer drugs, such as poor water solubility, low bioavailability, and unacceptable systemic toxicity (Bae *et al.,* 2009).

* *Corresponding Author*
Dr. Younsoo Bae, Department of Pharmaceutical Sciences,
College of Pharmacy, University of Kentucky,
789 South Limestone, Lexington, KY 40536-0596, USA
Phone: +1-859-323-6649, Fax: +1-859-257-7564

Despite these potential benefits, polymer nanoassemblies still need to be improved to control drug release in tumors for effective cancer chemotherapy because most anticancer drugs are designed to kill fast growing cancer cells by inhibiting signal pathways for cell survival during the cell division, and drug concentrations and timing of treatment are crucially important to maximize therapeutic efficacy (Kim *et al.,* 2002; Los *et al.,* 2003; Fulda *et al.,* 2006). Although polymer nanoassemblies that release drug slowly in the blood are expected to reduce systemic toxicity, they could also release drug too slowly to maintain therapeutic drug concentrations in tumor tissues (Fang *et al.,* 2011). These facts suggest that polymer nanoassemblies that accelerate drug release selectively in tumor tissues in a controlled manner may improve anticancer chemotherapy while reducing systemic toxicity.

Numerous approaches have been developed to control drug release from polymer nanoassemblies in response to external stimuli, such as pH, light, ultrasound, and heat alone or in combination (Sanvicens *et al.,* 2008; Bae *et al.,* 2009). Heat is particularly useful to control drug release because the body temperature is precisely regulated. Various methods are currently available to increase temperature in specific tissues locally, using

heating probes, plates, and inorganic nanomaterials (e.g. gold and iron oxide). Among these heating sources, iron oxide nanoparticles (IONPs) with superparamagnetic properties have drawn considerable attention because they can generate heat in the presence of an alternating magnetic field (AMF) (Neuberger *et al.*, 2005; Frimpong *et al.*, 2008; Frimpong *et al.*, 2010; Frimpong *et al.*, 2010; Meenach *et al.*, 2010; Meenach *et al.*, 2010; Satarkar *et al.*, 2010; He *et al.*, 2011; Satarkar *et al.*, 2011). IONPs can be also used as a T_2 contrast agent for magnetic resonance imaging (Bulte *et al.*, 2004). Such dual heating and imaging properties enable IONPs to be used for theranostics (Sumer *et al.*, 2008). However, IONPs have poor particle stability and agglomerate easily in aqueous solutions, causing toxicity to the human body (Mahmoudi *et al.*, 2009; Singh *et al.*, 2010; Soenen *et al.*, 2010; Mahmoudi *et al.*, 2011; Shen *et al.*, 2012). Particle stability of IONPs can be improved by surface modification or using solubilizer (e.g. surfactants and water soluble polymers) (Laurent *et al.*, 2008). Hydrophobic and ionic interactions have been identified as two major factors for block copolymers to self-assemble into polymer nanoassemblies, and regardless of the payload, particle size and stability are critically important for the polymer nanoassemblies to achieve successful tumor accumulation (Jain *et al.*, 2008; Lin *et al.*, 2008), yet critical issues, such as precipitation, agglomeration, and protein adsorption in vivo, are not resolved completely.

For these reasons, previous studies have been focused mainly on stabilizing IONP-loaded nanoparticles, and little efforts have been made to co-entrap IONPs and other therapeutic agents into a single nanoparticle for combination delivery (Harris *et al.*, 2003; Prompruk *et al.*, 2005; Kumagai *et al.*, 2007; Papaphilippou *et al.*, 2009; Konwarh *et al.*, 2010; Lee *et al.*, 2011; Schladt *et al.*, 2011; Xie *et al.*, 2011; Min *et al.*, 2012). In this study, we focus on the development of novel nanoparticle formulations for co-entrapment and co-delivery of IONPs and anticancer agents. We hypothesize that (1) stable and safe IONP-loaded nanoparticles can be prepared by precipitating IONPs inside polymer nanoassemblies, and (2) these nanoassemblies can be used to co-entrap therapeutic agents without compromising AMF-responsive heating profiles of the IONPs. To test these hypotheses, we have prepared and characterized the self-assembled nanoassemblies (SNAs) (Eckman *et al.*, 2012) and cross-linked nanoassemblies (CNAs) (Lee *et al.*, 2011; Ponta *et al.*, 2011; Scott *et al.*, 2011) from biocompatible poly(ethylene glycol)-poly(aspartate) block copolymers, entrapping IONPs and an anticancer drug (doxorubicin: DOX), and thus potentially accelerating drug release in tumors in response to AMF (Figure 1).

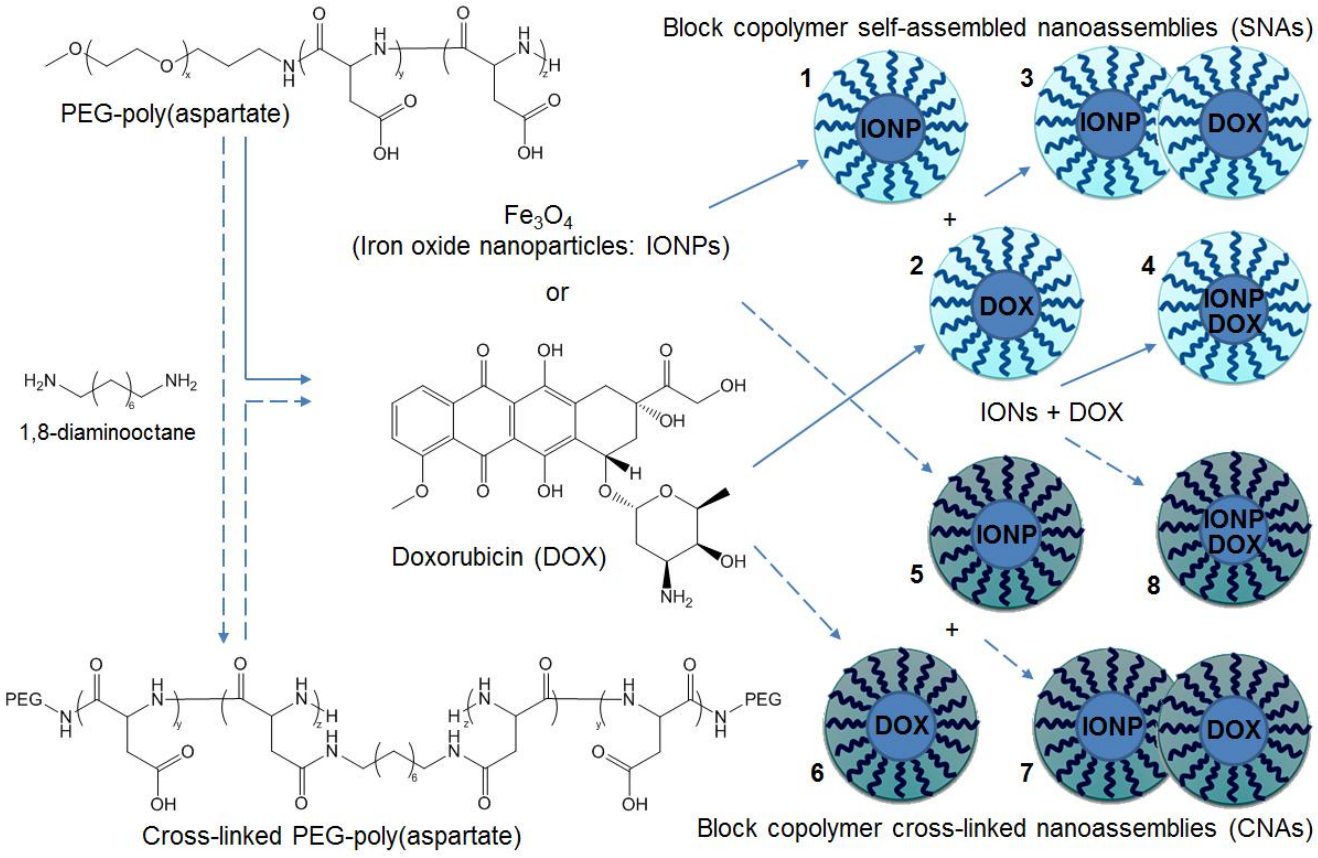

Fig 1. Polymer nanoassemblies used in this study to entrap IONPs and DOX in combination. Self-assembled nanoassemblies (SNAs, light blue) and cross-linked nanoassemblies (CNAs, dark green) were prepared from the same block copolymer [PEG-poly(aspartate)], and categorized into eight groups (1: IONP-loaded SNAs; 2: DOX-loaded SNAs; 3: Physical mixture of 1 and 2; 4: IONP/DOX co-entrapped SNAs; 5: IONP-loaded CNAs; 6: DOX-loaded CNAs; 7: Physical mixture of 5 and 6; and 8: IONP/DOX co-entrapped CNAs).

MATERIALS

Triphosgene, L-aspartic acid β-benzyl ester (BLA), N,N'-diisopropylcarbodiimide (DIC), N-hydroxysuccinimide (NHS), 4-(dimethylamino)pyridine (DMAP), anhydrous tetrahydrofuran (THF), anhydrous hexane, diethyl ether, dimethylsulfoxide (DMSO), phosphate buffer solution, phosphate buffered saline (PBS), 1,8-diaminooctane, doxorubicin hydrochloride (DOX-HCl), sodium hydroxide (NaOH), iron(II) chloride tetrahydrate, iron(III) chloride hexahydrate, and ammonium hydroxide (NH_4OH) were purchased from Sigma-Aldrich (USA). α-Methoxy-ω-amino poly(ethylene glycol) (PEG, 12 kDa) was purchased from NOF Corporation (Japan). Dialysis bags with molecular weight cut off (MWCO) 6 ~ 8 kDa and Slide-A-Lyzer G2 dialysis cassettes with MWCO 10 kDa, were purchased from Fisher Scientific (USA). SpectraPor 6 dialysis tubing with MWCO 50 kDa was purchased from Spectrum Labs (USA).

Block copolymer synthesis

Block copolymers were synthesized as reported previously (Bae *et al.,* 2005; Lee *et al.,* 2011). β-Benzyl-L-aspartate N-carboxy anhydride (BLA-NCA) was prepared as a monomer by reacting BLA with triphosgene (1.3 molar equivalent) in dry THF (50 ~ 100 mg/mL) at 45 °C until the solution turned clear. Anhydrous hexane was added to the solution to recrystallize BLA-NCA at -20 °C. The amino group of PEG was used to initiate polymerization of BLA-NCA in DMSO (50 mg/mL) at 45 °C under nitrogen for 2 days. The polymerization produced PEG-poly(β-benzyl L-aspartate) [PEG-PBLA], followed by precipitation in diethyl ether and freeze drying. The block copolymer composition was determined by proton nuclear magnetic resonance (^{1}H-NMR) spectra from PEG (3.5 ppm) and benzyl groups (7.3 ppm). The purity of block copolymers was determined by gel permeation chromatography (GPC, Shimadzu LC20), using PBS mobile phase and PEG standard.

Synthesis of CNAs

The CNAs were synthesized as previous reported with slight modification (Lee *et al.,* 2011). A two molar excess of NaOH was added to PEG-PBLA to remove the benzyl groups. Excess NaOH and other impurities were removed by dialysis. The solution was treated further with HCl to remove sodium salt, and freeze dried to collect PEG-poly(aspartate) [PEG-p(Asp)]. PEG-p(Asp) was dissolved in DMSO to a final concentration of 50 mg/mL. DIC, NHS, and DMAP were added to the solution at a molar ratio of 4:4:0.2 with respect to the number of the aspartate units of PEG-p(Asp). This solution was mixed with 1,8-diaminooctane [0.5 equivalent to carboxyl groups of p(Asp)] at 45 °C for 72 hours. CNAs were dialyzed against water, and collected by freeze drying.

Preparation and Characterization of Nanoassemblies Entrapping IONPs and DOX

Iron oxide (Fe_3O_4) was formed in the presence of either PEG-p(Asp) block copolymers or CNAs to simultaneously precipitate and entrap IONPs inside polymer nanoassemblies. Iron ions were added to PEG-p(Asp) and CNAs in a molar ratio of 1:1 (a ratio of 2:1 of Fe^{3+}:Fe^{2+}) with respect to carboxylic groups on the polymer chains. Ammonium hydroxide was then slowly added to the solution to precipitate the iron oxide, producing SNAs and CNAs entrapping IONPs (1 and 5 in Figure 1). IONPs that were formed outside of the polymer nanoassemblies aggregated and precipitated in the solutions while the IONPs entrapped inside the SNAs and CNAs remained soluble in the supernatant. Free IONPs as well as free ions (iron and sodium) were removed from the solution by centrifugation and dialysis. SNAs and CNAs entrapping IONPs were collected by freeze drying. DOX was entrapped in the polymer nanoassemblies through combined ionic and hydrophobic interactions. DOX-HCl was mixed with PEG-p(Asp) or CNAs in deionized water, followed by dialysis and ultracentrifugal filtration (30 kDa) until no free DOX was detected. SNAs and CNAs entrapping DOX were collected by freeze drying (2 and 6 in Figure 1). Polymer nanoassemblies co-entrapping IONPs and DOX were prepared by mixing DOX-HCl with the polymer nanoassemblies pre-loaded with IONPs. The products were collected by dialysis against water and freeze drying (4 and 8 in Figure 1). Physical mixtures of individual nanoassemblies entrapping either IONPs or DOX separately were prepared as comparison (3 and 7 in Figure 1). IONP loading yields were determined by weight % (wt%), using thermogravimetric analysis (TGA) instruments. Fourier transform infrared spectroscopy (FT-IR) was used to confirm the presence of polymers in IONP-loaded nanoassemblies. DOX entrapment yields were quantified by UV-Vis absorbance measurements at 480 nm. Particle sizes of all samples were determined by dynamic light scattering (DLS) measurements (Zetasizer Nano ZS, Malvern). Data are shown as average from triplicate measurements ± standard deviation (SD).

Heating of IONP-Loaded Polymer Nanoassemblies

Heating capability of IONP-loaded SNAs and CNAs was determined in the presence of AMF, using a custom made induction power supply (Taylor Winfield, MMF-3-135/400-2). IONP-loaded nanoassemblies were dissolved in deionized water at 2 mg/mL and placed in a 1.5 mL microtube. The solution was placed inside the coil of the AMF unit, using a Luxtron FOT lab kit temperature probe (LumaSense Technologies) to monitor the overall solution temperature of the sample. A baseline temperature was obtained from a blank solution for 30 seconds and the AMF was switched on at 70% power, corresponding to a field strength of approximately 59.3 kA/m at 300 kHz. The temperature was then monitored for 15 minutes. Images of the AMF-induced heating of the IONP-loaded nanoassemblies were captured using an infrared (IR) camera (SC4000, FL-IR Systems).

IONP-loaded nanoassemblies in water (2 mg/mL) were placed in a 35 mm culture dish and set on top of the AMF coil (33.4 kA/m at 300 kHz) for taking IR images. The change in the heating profile based on IONP concentration was evaluated

through the application of AMF to varying IONP-CNA concentrations. The total IONP-CNA concentrations were set at 1, 2.5, and 5 mg/mL based on IONPs, followed by the application of AMF. The initial temperature was held at either 25ºC or 37ºC by a customized warming chamber.

Evaluation of Temperature Dependent Drug Release

The influence of heat on drug release from polymer nanoassemblies was determined by evaluating SNAs and CNAs that co-entrapping IONPs and DOX. The polymer nanoassemblies (300 µL of 2 mg DOX/mL) were put in three dialysis cassettes (Slide-A-Lyzer G2, MWCO 10 kDa, Thermo Scientific, USA). The sample solutions were dialyzed in excess phosphate buffer solutions (pH 7.4, 20 mM) while the temperature was maintained at either 37ºC or 45ºC. An aliquot of 20 µL was taken out of each dialysis cassette at 0, 0.5, 1, 2, 4, and 6 hours. DOX remaining in the dialysis cassettes were quantified by UV/Vis absorbance at 480 nm. All experiments were performed in triplicate.

Stability of Nanoassemblies

The stability of SNAs and CNAs co-entrapping IONPs and DOX was investigated over a period of 5 days. The polymer nanoassemblies were dissolved in deionized water at 2 mg/mL, and added to a disposable capillary tube. The nanoparticles were stored at room temperature and the particle size was observed by DLS in triplicate on days 1, 3, and 5.

RESULTS AND DISCUSSION

Synthesis of block copolymers and CNAs

^{1}H-NMR analysis determined that polymerization of BLA-NCA produced PEG-PBLA with 28 aspartate repeating units. GPC was used to confirm the purity of the polymer and the cross-linking of PEG-p(Asp) with 1,8-diaminooctane. A single peak of PEG-p(Asp) on GPC shifted to a higher molecular range with a shorter elution time after the cross-linking reaction (Figure 2).

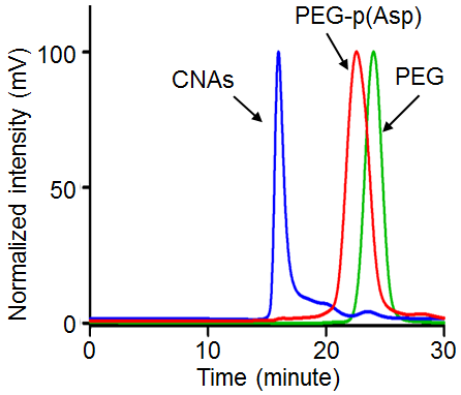

Fig 2. GPC spectra of PEG (12 kDa), PEG-p(Asp) block copolymers, and CNAs.

A relatively narrow distribution of the CNAs was also observed with a Mw/Mn of 1.14. Neither unreacted polymers nor impurities were detected after purification of CNAs. The average molecular weight of CNAs was approximately 129 kDa, indicating that one CNA particle contained 7 ~ 8 block copolymer chains. These results were consistent with what we observed previously (Lee *et al.*, 2011; Eckman *et al.*, 2012).

Entrapment of IONPs and DOX

IONPs are normally stabilized with citric acid or surfactants to avoid agglomeration (Laurent *et al.*, 2008). In this study, we used PEG-p(Asp) or CNAs as stabilizers to simultaneously prepare and entrap IONPs inside polymer nanoassemblies. This approach allowed us to control the particle size of polymer nanoassemblies within a clinically relevant range (< 100 nm). Successful incorporation of IONPs into the polymer nanoassemblies was achieved at a 2:1 ratio of Fe^{3+}:Fe^{2+} in solution with an equivalent amount of carboxyl groups of PEG-p(Asp) or CNAs. The solution containing iron ions and polymers formed dark brown precipitates immediately after NH_4OH was added. IONPs entrapped in polymer nanoassemblies were readily separated from free IONPs by centrifugation as the entrapped IONPs remained soluble in aqueous solutions. The supernatant was collected and dialyzed to remove unreacted iron ions and other impurities, followed by freeze drying.

DOX was also successfully entrapped in either empty or IONP-loaded nanoassemblies. DOX and PEG-p(Asp) block copolymers formed SNAs spontaneously as they were mixed in deionized water. The amount of DOX loaded into nanoassemblies was quantified by UV-Vis absorbance at 480 nm (25.6 wt%). FT-IR was used to confirm IONP incorporation into polymer nanoassemblies (Figure 3).

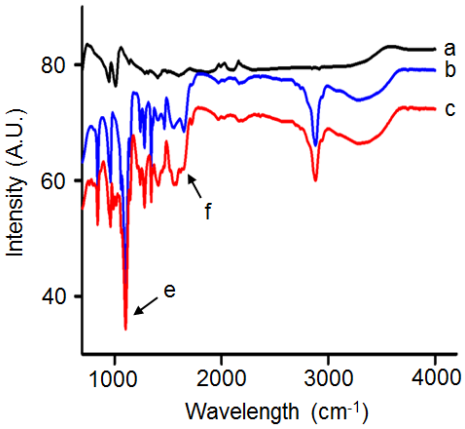

Fig 3. FT-IR characterization (a: IONPs; b: IONP-loaded polymer nanoassemblies; c: IONP/DOX co-entrapped polymer nanoassemblies; e: ether peak at 1,100 cm-1; and f: amide peak at 1,650 cm-1).

IONPs are dark brown materials, which were easily detected by color in our IONP-loaded polymer nanoassemblies after purification. The ether peak at 1,100 cm^{-1} and amide at 1,650 cm^{-1} indicated the presence of PEG and p(Asp), respectively. These unique polymer peaks appeared in both IONP-loaded nanoassemblies and nanoassemblies co-entrapping IONP and

DOX while the IONPs alone lacked the peaks of interest. It is possible that unencapsulated IONPs and free block copolymers could result in a similar FTIR trace. However, unencapsulated IONPs precipitate easily and cannot be present in aqueous solutions, following several purification steps used for IONP-loaded nanoparticles. TGA confirmed that polymer nanoassemblies contained 26 wt% of IONPs (Figure 4). The particle sizes of nanoassemblies are summarized in Table 1, indicating that the average diameter was less than 100 nanometers regardless of the nanoassembly composition.

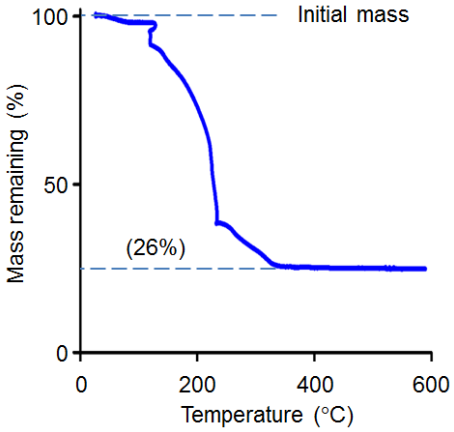

Fig 4. TGA characterization and the IONP loading yield in CNAs.

Table 1. Size comparison of polymer nanoassemblies entrapping IONPs and DOX.

Samples	Diameter ± SD (nm)
IONP-loaded SNAs	34.4 ± 6.0
DOX-loaded SNAs	57.7 ± 3.3
IONP/DOX co-entrapped SNAs	54.3 ± 6.5
Physical mixture of IONP- and DOX-loaded SNAs	46.0 ± 8.8
IONP-loaded CNAs	64.0 ± 10.4
DOX-loaded CNAs	70.6 ± 4.7
IONP/DOX co-entrapped CNAs	75.0 ± 11.0
Physical mixture of IONP- and DOX-loaded CNAs	67.5 ± 10.9

Heating profile of IONP-loaded polymer nanoassemblies

The heating ability of IONPs inside polymer nanoassemblies was investigated using a temperature probe and an IR camera in the presence of AMF. In Figure 5A, nanoparticle solutions (1 ~ 5 mg IONP/mL) reached the hyperthermic temperature range (40 ~ 42ºC) in 600 seconds in the presence of AMF. As the concentration of IONP-loaded CNAs increased, the observed solution temperature also increased. However, the temperature of solution at 1 mg IONP/mL was always lower than nanoassembly solutions at higher IONP concentrations (2.5 or 5 mg/mL) and showed no further increase over time. It is noticeable that initial solution temperatures (37ºC vs 25ºC) did not change the heating rate of polymer nanoassemblies (Figure 5A and 5B). These results indicate that the concentration of IONPs in the solution is the major factor that affects heating profiles of IONP-loaded polymer nanoassemblies. Figure 5 B indicates that polymer nanoassemblies retain the heating profile in the absence (a) and presence (b) of drug payloads (DOX). IR images show that the heating efficiency of IONPs inside polymer nanoassemblies changed substantially inside and over the AMF coil (c and d in Figure 5B).

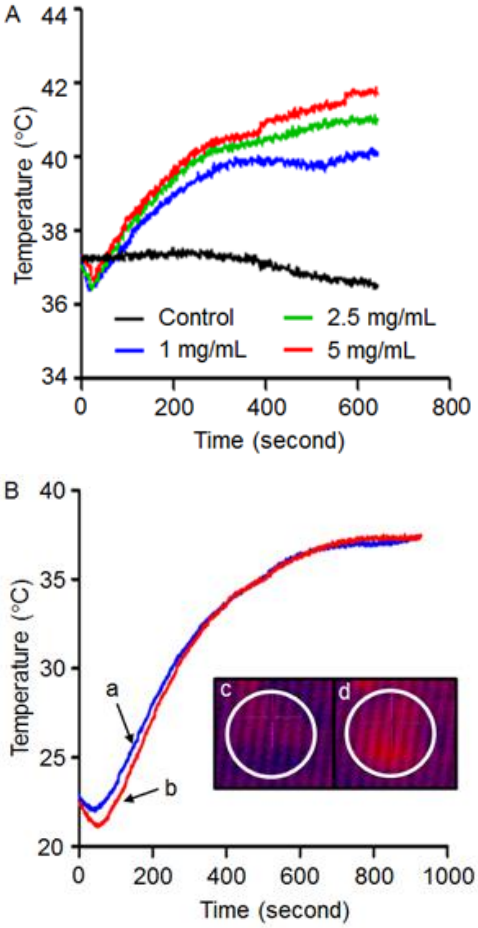

Fig 5. Heating profiles of IONP-loaded CNAs. (A) The changes in solution temperature upon the application of AMF were observed at different particle concentrations (control: deionized water). (B) Effects of drug payloads on the heating profile were also investigated (a: IONP-loaded CNAs alone; b: IONP/DOX co-entrapped CNAs; c: infrared thermal image of a blank; and d: thermal images of IONP-loaded CNAs. AMF generating coils are shown in white circles.)

These results demonstrate the ability to tune the heat produced by the IONP-loaded nanoassemblies and allow adjustments in order to minimize heat damage to other normal tissue outside of the accumulated area while maximizing the effectiveness of the treatment. In addition, these remotely heatable nanoassemblies can carry drug payloads at the same time without compromising the heating profiles, allowing unique hyperthermia and chemotherapy combination. We envision that, by selectively applying an AMF to the area of interest after the nanoparticles have accumulated in the tumor, heat and the accelerated drug release can be confined to the tumor and aid in reducing non-specific side effects. Remote heating of IONP-loaded polymer nanoassemblies is useful not only for drug release acceleration but also for heat-induced therapies such as hyperthermia or thermoablation (Meenach *et al.*, 2010). The range of temperature

that these polymer nanoassemblies can modulate is still dependent largely on the concentration of the nanoassemblies and power of AMF. We observed a significant decrease in heating efficiency between polymer nanoassemblies in and over the AMF coil. The optimal design of AMF-generating devices might improve the heating of polymer nanoassemblies *in vivo*, allowing focused heating for drug release acceleration and therapy. Recent work has demonstrated IONPs possess a therapeutic effect outside of the heating of the cancer cells. Magnetic nanoparticles were shown to reduce cell viability to 2 ~ 5% when exposed to an alternating magnetic field even without raising the solution temperature (Wust *et al.*, 2002; Marcos-Campos *et al.*, 2011). Therefore, IONP/DOX loaded polymer nanoassemblies may exhibit a beneficial therapeutic effect as AMF-responsive nanomaterials *in vivo*, although potential effects of AMF and magnetic fields in vivo (e.g. heating of tissue for 10 minutes as tested in this study) are not fully understood yet (Lednev 1991; Walleczek 1992; Grissom 1995).

Temperature-dependent drug release

Drug release patterns from polymer nanoassemblies co-entrapping IONPs and DOX were determined at 37ºC and 45ºC (pH 7.4, 20 mM PBS), corresponding to the physiological and hyperthermic condition, respectively. Both SNAs and CNAs accelerated drug release as the temperature increased from 37ºC to 45ºC, although the difference was subtle (Figure 6).

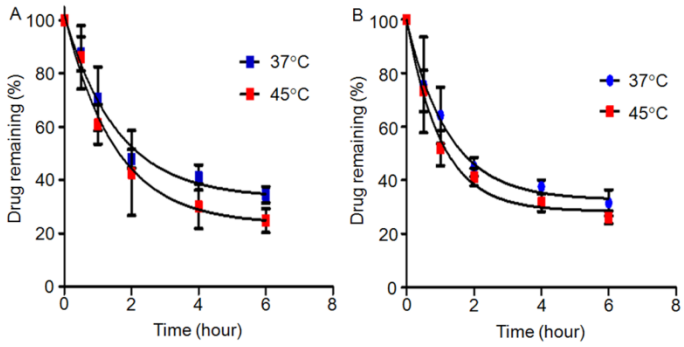

Fig 6. The influence of temperature on drug release patterns from SNAs (A) and CNAs (B). All data points are the average of three measurements ± standard deviation.

Such accelerated drug release gradually slowed down after 2 hours, following pseudo-zero order drug release in the early stage. These bi-modal drug release patterns are expected to fine-tune optimal drug concentrations in tumors in future in vivo applications. Although an increased temperature (e.g. 45ºC as tested in this study) could damage normal tissues, pinpoint hyperthermia using our IONP-loaded CNAs would reduce such potential risks. In addition, AMF can switch on and off the heating and accelerating drug release in a remotely controlled manner, which will further reduce potential toxicity by hyperthermia with IONP-loaded nanoassemblies.

Interestingly, there was no significant difference between SNAs and CNAs in the drug release profile. These results imply that polymer nanoassemblies entrapping IONPs may have a similar core environment, where IONPs occupy the center of core and DOX gets weakly bound to the core. It is also possible that drug molecules were indeed entrapped inside the nanoassembly core, yet failed to come out as more than 20% of drugs still remained in the nanoassemblies. Therefore, accelerated drug release is likely attributed to temperature-dependent changes in hydration of PEG of the particles, affecting mainly the drugs along the boundary region between the core and shell. Hydration is one of the factors that influence molecular diffusion in a layer and matrix made of PEG. PEG is a flexible polymer chain, but SNAs and CNAs tether PEG chains to an IONP-loaded core, providing a nanoscale PEG compartment in the shell, a physical barrier that drug molecules need to go through. Therefore, IONPs generating heat in the presence of AMF may enhance molecular diffusion of DOX from the polymer nanoassemblies, although we were unable to direct observe such a phenomenon due to the technical issue to apply AMF to nanoparticles inside dialysis cassettes in a large water bath (> 5 L).

Stability of Polymer Nanoassemblies

The stability of polymer nanoassemblies co-entrapping IONPs and DOX (co-entrapped type) was evaluated in deionized water over five days, while preparing a mixed solution of nanoassemblies entrapping IONPs or DOX separately (physically mixed type) as a control. In Figure 7A, the particle size of physically mixed SNAs decreased time-dependently, and the observed particle size decreased by 63% over a period of 5 days (a, b, and c). Co-entrapped type SNAs retained their particle size for 5 days (d, e, and f in Figure 7A). However, both physically mixed and co-entrapped SNAs generated precipitates in solutions. The particle sizes of CNAs remained unchanged in physically mixed and co-entrapped types (Figure 7B).

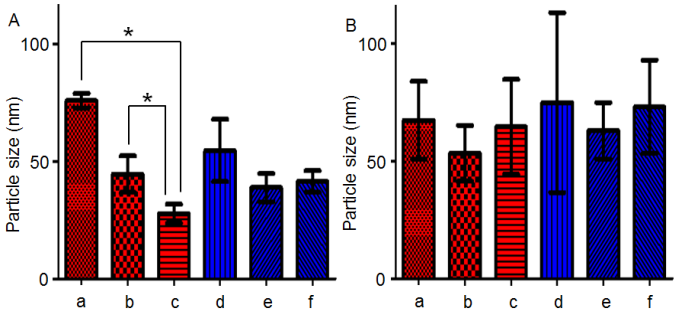

Fig 7. Time-dependent changes in particle sizes of SNAs (A) and CNAs (B) entrapping IONPs and DOX (a: Physically mixed type on day 1; b: Physically mixed type on day 3; c: Physically mixed type on day 5; d: Co-entrapped type on day 1; e: Co-entrapped type on day 3; and f: Co-entrapped type on day 5). All points are shown the average of three measurements ± standard deviation. (*: $P < 0.05$).

No precipitates were observed in CNAs, suggesting that IONPs and DOX were entrapped effectively in polymer nanoassemblies due to the cross-linked core. Interestingly the polymer nanoassemblies co-entrapping IONPs and DOX (both SNAs and CNAs) showed improved stability with no significant

change in the observed size. One possible reason is that IONPs could act as a cross-linker and hold multiple block copolymers together to prevent dissociation. In a physically mixed formulation, CNAs showed greater particle stability than SNAs. CNAs with enhanced particle stability can be also used to introduce other functional groups without compromising the particle stability. In fact, particle stability is an emerging issue for nanoparticulate drug carriers as numerous approaches have been used to control drug release by introducing functional groups that are sensitive to heat, light, and pH (Bae *et al.*, 2009). Previous studies employed a method through which pre-formed iron oxide particles were entrapped in the polymer matrice, particles, or complexes (Kumagai *et al.*, 2007; Sanvicens *et al.*, 2008; Obena *et al.*, 2011). On the contrary, we prepared cross-linked nanoassemblies first, reacted the nanoassemblies with iron ions, and prepared IONP-loaded nanoassemblies in a single pot. This method, co-precipitating Fe_3O_4 iron oxides inside the nanoassemblies directly, was confirmed efficient and convenient to prepare IONP-loaded nanoparticles with homogeneous particle sizes and enhanced particle stability.

CONCLUSION

Block copolymer self-assembled and cross-linked nanoassemblies (SNAs and CNAs) were prepared in this study to develop novel nanoscale carriers for the delivery of iron oxide nanoparticles (IONPs) and anticancer drug (DOX) in combination to disease sites in the body (e.g. tumors). Polymer nanoassemblies entrapping IONPs and DOX were successfully prepared by precipitating iron oxide inside the polymer nanoassemblies, and the particle sizes were < 100 nm, which is clinically relevant for macromolecules to accumulate in tumor tissues. IONP-loaded SNAs and CNAs generated heat in the presence of an alternating magnetic field (AMF), and the concentrations of IONPs in a solution played a major role in controlling the temperature. Heating properties of IONP-loaded nanoparticles were retained even after entrapping DOX in the SNAs and CNAs. Drug release from the polymer nanoassemblies was accelerated as temperature increased, yet the change was subtle presumably because IONPs occupy the core of nanoassemblies while drug molecules were weakly bound to the core or entrapped in the shell. Despite similar drug release patterns, CNAs showed greater particle stability than SNAs during storage in solutions, suggesting that CNAs would be a suitable candidate to further develop IONP/DOX co-entrapped polymer nanoassemblies for future applications, such as AMF-mediated remote heating and triggered drug release in vivo.

Acknowledgments

DS and MD acknowledge the financial support from a NCI-CNTC postdoctoral and pre-doctoral traineeship, respectively, and the project described was supported by Grant Number 5R25CA153954 from the National Cancer Institute. YB acknowledges support from the Kentucky Lung Cancer Research Program and the NSF-REU at the University of Kentucky.

REFERENCES

Bae Y., Jang W.-D., Nishiyama N., Fukushima S., and Kataoka K. Multifunctional polymeric micelles with folate-mediated cancer cell targeting and pH-triggered drug releasing properties for active intracellular drug delivery. *Mol BioSyst* 2005; *3*: 242-250.

Bae Y., and Kataoka K. Intelligent polymeric micelles from functional poly(ethylene glycol)-poly(amino acid) block copolymers. *Adv Drug Deliver Rev* 2009; *10*: 768-784.

Bae Y., and Kataoka K. Intelligent polymeric micelles from functional poly(ethylene glycol)-poly(amino acid) block copolymers. *Adv Drug Deliv Rev* 2009; *10*: 768-784.

Bulte J.W.M., and Kraitchman D.L. Iron oxide MR contrast agents for molecular and cellular imaging. *NMR in Biomedicine* 2004; *7*: 484-499.

Eckman A.M., Tsakalozou E., Kang N.Y., Ponta A., and Bae Y. Drug Release Patterns and Cytotoxicity of PEG-poly(aspartate) Block Copolymer Micelles in Cancer Cells. *Pharm Res* 2012;

Fang J., Nakamura H., and Maeda H. The EPR effect: Unique features of tumor blood vessels for drug delivery, factors involved, and limitations and augmentation of the effect. *Adv Drug Deliver Rev* 2011; *3*: 136-151.

Frimpong R.A., Dou J., Pechan M., and Hilt J.Z. Enhancing remote controlled heating characteristics in hydrophilic magnetite nanoparticles via facile co-precipitation. *J Magn Magn Mater* 2010; *3*: 326-331.

Frimpong R.A., and Hilt J.Z. Magnetic nanoparticles in biomedicine: synthesis, functionalization and applications. *Nanomedicine* 2010; *9*: 1401-1414.

Frimpong R.A., and Hilt J.Z. Poly(n-isopropylacrylamide)-based hydrogel coatings on magnetite nanoparticles via atom transfer radical polymerization. *Nanotechnology* 2008; *17*:

Fulda S., and Debatin K.M. Resveratrol modulation of signal transduction in apoptosis and cell survival: a mini-review. *Cancer Detect Prev* 2006; *3*: 217-223.

Grissom C.B. Magnetic-Field Effects in Biology - a Survey of Possible Mechanisms with Emphasis on Radical-Pair Recombination. *Chem Rev* 1995; *1*: 3-24.

Harris L.A., Goff J.D., Carmichael A.Y., Riffle J.S., Harburn J.J., St Pierre T.G., and Saunders M. Magnetite nanoparticle dispersions stabilized with triblock copolymers. *Chem Mater* 2003; *6*: 1367-1377.

He Z.W., Satarkar N., Xie T., Cheng Y.T., and Hilt J.Z. Remote Controlled Multishape Polymer Nanocomposites with Selective Radiofrequency Actuations. *Adv Mater* 2011; *28*: 3192-+.

Ishida O., Maruyama K., Sasaki K., and Iwatsuru M. Size-dependent extravasation and interstitial localization of polyethyleneglycol liposomes in solid tumor-bearing mice. *Int J Pharm* 1999; *1*: 49-56.

Jain T.K., Richey J., Strand M., Leslie-Pelecky D.L., Flask C.A., and Labhasetwar V. Magnetic nanoparticles with dual functional properties: drug delivery and magnetic resonance imaging. *Biomaterials* 2008; *29*: 4012-4021.

Khemtong C., Kessinger C.W., and Gao J. Polymeric nanomedicine for cancer MR imaging and drug delivery. *Chem Commun* 2009; *24*: 3497-3510.

Kim R., Tanabe K., Uchida Y., Emi M., Inoue H., and Toge T. Current status of the molecular mechanisms of anticancer drug-induced apoptosis. The contribution of molecular-level analysis to cancer chemotherapy. *Cancer Chemother Pharmacol* 2002; *5*: 343-352.

Konwarh R., Saikia J.P., Karak N., and Konwar B.K. 'Poly(ethylene glycol)-magnetic nanoparticles-curcumin' trio: Directed morphogenesis and synergistic free-radical scavenging. *Colloid Surface B* 2010; *2*: 578-586.

Kumagai M., Imai Y., Nakamura T., Yamasaki Y., Sekino M., Ueno S., Hanaoka K., Kikuchi K., Nagano T., Kaneko E., Shimokado K., and Kataoka K. Iron hydroxide nanoparticles coated with poly(ethylene glycol)-poly(aspartic acid) block copolymer as novel magnetic resonance contrast agents for in vivo cancer imaging. *Colloid Surface B* 2007; *1-2*: 174-181.

Laurent S., Forge D., Port M., Roch A., Robic C., Elst L.V., and Muller R.N. Magnetic iron oxide nanoparticles: Synthesis, stabilization, vectorization, physicochemical characterizations, and biological applications. *Chem Rev* 2008; *6*: 2064-2110.

Lednev V.V. Possible Mechanism for the Influence of Weak Magnetic-Fields on Biological-Systems. *Bioelectromagnetics* 1991; *2*: 71-75.

Lee H.J., and Bae Y. Cross-Linked Nanoassemblies from Poly(ethylene glycol)-poly(aspartate) Block Copolymers as Stable Supramolecular Templates for Particulate Drug Delivery. *Biomacromolecules* 2011; *7*: 2686-2696.

Lee H.J., Ponta A., and Bae Y. Polymer nanoassemblies for cancer treatment and imaging. *Therapeutic Delivery* 2010; *6*: 803-817.

Lee S.J., Min K.H., Lee H.J., Koo A.N., Rim H.P., Jeon B.J., Jeong S.Y., Heo J.S., and Lee S.C. Ketal Cross-Linked Poly(ethylene glycol)-Poly(amino acid)s Copolymer Micelles for Efficient Intracellular Delivery of Doxorubicin. *Biomacromolecules* 2011; *4*: 1224-1233.

Lin M.M., Kim do K., El Haj A.J., and Dobson J. Development of superparamagnetic iron oxide nanoparticles (SPIONS) for translation to clinical applications. *IEEE T Nanobiosci* 2008; *4*: 298-305.

Los M., Burek C.J., Stroh C., Benedyk K., Hug H., and Mackiewicz A. Anticancer drugs of tomorrow: apoptotic pathways as targets for drug design. *Drug Discov Today* 2003; *2*: 67-77.

Maeda H., Wu J., Sawa T., Matsumura Y., and Hori K. Tumor vascular permeability and the EPR effect in macromolecular therapeutics: a review. *J Control Release* 2000; *1-2*: 271-284.

Mahmoudi M., Laurent S., Shokrgozar M.A., and Hosseinkhani M. Toxicity Evaluations of Superparamagnetic Iron Oxide Nanoparticles: Cell "Vision" versus Physicochemical Properties of Nanoparticles. *ACS Nano* 2011; *9*: 7263-7276.

Mahmoudi M., Simchi A., Milani A.S., and Stroeve P. Cell toxicity of superparamagnetic iron oxide nanoparticles. *J Colloid Interface Sci* 2009; *2*: 510-518.

Marcos-Campos I., Asin L., Torres T.E., Marquina C., Tres A., Ibarra M.R., and Goya G.F. Cell death induced by the application of alternating magnetic fields to nanoparticle-loaded dendritic cells. *Nanotechnology* 2011; *20*: 205101.

Matsumura Y., and Maeda H. A new concept for macromolecular therapeutics in cancer chemotherapy: mechanism of tumoritropic accumulation of proteins and the antitumor agent smancs. *Cancer Res* 1986; *12 Pt 1*: 6387-6392.

Meenach S.A., Anderson K.W., and Hilt J.Z. Synthesis and Characterization of Thermoresponsive Poly(ethylene glycol)-Based Hydrogels and Their Magnetic Nanocomposites. *J Polym Sci Pol Chem* 2010; *15*: 3229-3235.

Meenach S.A., Hilt J.Z., and Anderson K.W. Poly(ethylene glycol)-based magnetic hydrogel nanocomposites for hyperthermia cancer therapy. *Acta Biomater* 2010; *3*: 1039-1046.

Min K.H., Lee H.J., Kim K., Kwon I.C., Jeong S.Y., and Lee S.C. The tumor accumulation and therapeutic efficacy of doxorubicin carried in calcium phosphate-reinforced polymer nanoparticles. *Biomaterials* 2012; *23*: 5788-5797.

Neuberger T., Schöpf B., Hofmann H., Hofmann M., and von Rechenberg B. Superparamagnetic nanoparticles for biomedical applications: Possibilities and limitations of a new drug delivery system. *J Magn Magn Mater* 2005; *1*: 483-496.

Obena R.P., Lin P.C., Lu Y.W., Li I.C., del Mundo F., Arco S., Nuesca G.M., Lin C.C., and Chen Y.J. Iron oxide nanomatrix facilitating metal ionization in matrix-assisted laser desorption/ionization mass spectrometry. *Anal Chem* 2011; *24*: 9337-9343.

Papaphilippou P., Loizou L., Popa N.C., Han A., Vekas L., Odysseos A., and Krasia-Christoforou T. Superparamagnetic Hybrid Micelles, Based on Iron Oxide Nanoparticles and Well-Defined Diblock Copolymers Possessing beta-Ketoester Functionalities. *Biomacromolecules* 2009; *9*: 2662-2671.

Ponta A., Akter S., and Bae Y. Degradable cross-linked nanoassemblies as drug carriers for heat shock protein 90 inhibitor 17-N-allylamino-17-demethoxygeldanamycin. *Pharmaceuticals* 2011; 1281-1292.

Prompruk K., Govender T., Zhang S., Xiong C.D., and Stolnik S. Synthesis of a novel PEG-block-poly(aspartic acid-stat-phenylalanine) copolymer shows potential for formation of a micellar drug carrier. *Int J Pharm* 2005; *1-2*: 242-253.

Sanvicens N., and Marco M.P. Multifunctional nanoparticles--properties and prospects for their use in human medicine. *Trends Biotechnol* 2008; *8*: 425-433.

Satarkar N.S., Biswal D., and Hilt J.Z. Hydrogel nanocomposites: a review of applications as remote controlled biomaterials. *Soft Matter* 2010; *11*: 2364-2371.

Satarkar N.S., Meenach S.A., Anderson K.W., and Hilt J.Z. Remote Actuation of Hydrogel Nanocomposites: Heating Analysis, Modeling, and Simulations. *AIChE J* 2011; *4*: 852-860.

Schladt T.D., Schneider K., Schild H., and Tremel W. Synthesis and bio-functionalization of magnetic nanoparticles for medical diagnosis and treatment. *Dalton T* 2011; *24*: 6315-6343.

Scott D., Rohr J., and Bae Y. Nanoparticulate formulations of mithramycin analogs for enhanced cytotoxicity. *Int J Nanomed* 2011; 2757-2767.

Shen M., Cai H., Wang X., Cao X., Li K., Wang S.H., Guo R., Zheng L., Zhang G., and Shi X. Facile one-pot preparation, surface functionalization, and toxicity assay of APTS-coated iron oxide nanoparticles. *Nanotechnology* 2012; *10*: 105601.

Singh N., Jenkins G.J., Asadi R., and Doak S.H. Potential toxicity of superparamagnetic iron oxide nanoparticles (SPION). *Nano Rev* 2010;

Soenen S.J., and De Cuyper M. Assessing iron oxide nanoparticle toxicity in vitro: current status and future prospects. *Nanomedicine* 2010; *8*: 1261-1275.

Sumer B., and Gao J.M. Theranostic nanomedicine for cancer. *Nanomedicine* 2008; *2*: 137-140.

Torchilin V. Tumor delivery of macromolecular drugs based on the EPR effect. *Adv Drug Deliver Rev* 2011; *3*: 131-135.

Walleczek J. Electromagnetic-Field Effects on Cells of the Immune-System - the Role of Calcium Signaling. *Faseb J* 1992; *13*: 3177-3185.

Wust P., Hildebrandt B., Sreenivasa G., Rau B., Gellermann J., Riess H., Felix R., and Schlag P.M. Hyperthermia in combined treatment of cancer. *Lancet Oncol* 2002; *8*: 487-497.

Xie J., Liu G., Eden H.S., Ai H., and Chen X. Surface-engineered magnetic nanoparticle platforms for cancer imaging and therapy. *Acc Chem Res* 2011; *10*: 883-892.

How to cite this article:

Daniel Scott, Yihwa Beabout, Robert J. Wydra, Mo Dan, Robert Yokel, J. Zach Hilt and Younsoo Bae. Block Copolymer Self-assembled and Cross-linked Nanoassemblies for Combination Delivery of Iron Oxide and Doxorubicin. J App Pharm Sci, 2013; 3 (06): 021-028.